

## Effect of oxygen deficiency on the normal and superconducting properties of $\text{YBa}_2\text{Cu}_3\text{O}_{7-\delta}$

S. I. Park, C. C. Tsuei, and K. N. Tu

*IBM Thomas J. Watson Research Center, Yorktown Heights, New York 10598*

(Received 2 October 1987)

Resistivity and structural studies on oxygen-deficient single-phase samples of polycrystalline  $\text{YBa}_2\text{Cu}_3\text{O}_{7-\delta}$  are presented. The oxygen content is controlled through annealing in He atmosphere. By analyzing the behavior of the normal-state resistivity as a function of  $\delta$  in terms of one-dimensional conduction, we provide evidence that one-dimensional CuO chains are responsible for the dominant normal-state conduction and the superconductivity at 91 K. The effects of oxygen deficiency on the superconducting properties are also discussed.

The recent discoveries of high- $T_c$  superconducting Cu oxides have led to intense theoretical and experimental activities on these materials.<sup>1,2</sup> In  $\text{YBa}_2\text{Cu}_3\text{O}_7$  oxide, its ability to sustain a large number of vacancies has enabled one to study its properties as a function of vacancy concentrations.<sup>3-8</sup> Although the importance of the one-dimensional Cu-O chain structure for high  $T_c$  was recognized from neutron-diffraction studies,<sup>3,4</sup> the exact role of the chains is not yet clear. Specifically, it is not clear whether the chains are the primary source of superconductivity [i.e., superconductivity is one-dimensional (1D) in nature] or they serve a secondary role by, for example, stabilizing the crystal structure or controlling the density of holes in the system. In the latter case, it is believed that 2D CuO sheets in between the Y and Ba layers are responsible for superconductivity (i.e., superconductivity is 2D in nature). Due to the existence of a large amount of twinning in this material, even the experimental observation<sup>9</sup> of isotropic conduction in the  $a$ - $b$  plane does not rule out the possibility of 1D superconductivity.

In many studies of oxygen-deficient Y-Ba-Cu-O,  $T_c$  was used as the prime parameter to characterize the material while the normal-state resistivity was largely ignored. Yet, superconducting and normal-state transport properties are intimately related since most likely the same carriers are responsible for both properties. Therefore, understanding normal-state conduction will shed light on the microscopic details of superconductivity in this material. In this paper, we report a systematic study of normal and superconducting transport and structural properties in oxygen-deficient Y-Ba-Cu-O samples. We show that all the salient features in the normal-state transport behavior can be explained in terms of 1D conduction and conclude that superconductivity at 91 K is a result of electronically coupled 1D chains.

The samples are prepared from a mixture of powders of BaO,  $\text{Y}_2\text{O}_3$ , and CuO. The right proportion is mixed, pressed into disks, and sintered at 950°C for 40 h in air. The samples are then cooled down to 750°C and held for 20 h in flowing oxygen atmosphere. The samples are furnace cooled to room temperature in about 7 h. The as-prepared samples are assumed to contain seven oxygen atoms per cell.<sup>10</sup> The samples are dry cut by a diamond wheel saw into bars of 1.2 mm × 1.2 mm × 1 cm. The oxygen-deficient samples are prepared by annealing the

bars in flowing He atmosphere at temperatures ranging from 420–500°C for 1–6 h and furnace cooling in He to 100°C in about 5 h. In some samples, the oxygen loss is estimated by weighing the bar before and after the He-annealing procedure. A typical bar weighted about 60 mg and a change in weight to within 0.05% was measurable. A concurrent study on oxygen diffusion in Y-Ba-Cu-O during the He annealing indicates that the removal of the oxygen is not diffusion limited but interface reaction limited so that the individual grains lose oxygen linearly with annealing time and maintain a homogeneous oxygen distribution.<sup>11</sup>

Figure 1 shows the resistivity  $\rho$  versus temperature  $T$

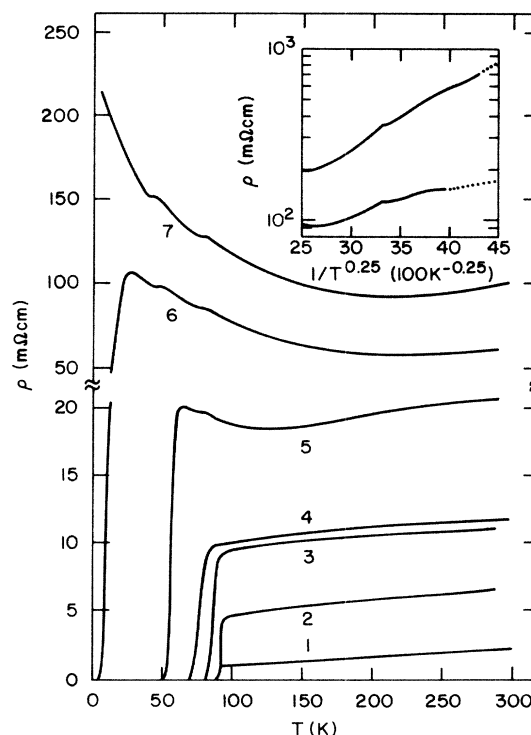


FIG. 1. Resistivity  $\rho$  as a function of temperature for several He-annealed samples. The nominal oxygen content for some samples are (1) 7.0, (2) 6.83, (4) 6.71, (5) 6.56, and (6) 6.42. The inset shows the activated hopping conduction for sample (7) and one other.

curves for a few typical samples. Basically two groups of samples exist, those (numbered 1–4) that show metallic behavior and those (numbered 5–7) that show a region of negative temperature coefficient of resistance (TCR). Typically, the samples with (without) the region of negative TCR have oxygen content [O] less (greater) than about 6.7. We observe two noticeable features in Fig. 1: first, the residual resistivity (defined by extrapolating the linear portion of  $\rho$  vs  $T$  curve to zero temperature) increases rapidly with increasing annealing time and second, the samples (numbered 6 and 7) with bulk  $T_c < \sim 45$  K exhibit double resistance dips at temperature  $\sim 77$  and  $\sim 45$  K before becoming superconducting (or insulating) at lower temperatures. One peculiarity is that the amount of resistance drop at the two temperatures is equal in magnitude for each sample. The localization portion of the resistivity curves can be well fitted to an activated hopping term with exponent 0.25 (see inset of Fig. 1).

Figure 2 shows the result of *in situ* resistance measurement during an annealing procedure at 396 °C. The measurement was done by the Van der Pauw method on a sample of size of 13 mm  $\times$  5 mm  $\times$  1.2 mm. The ambient of the furnace was changed from He to air, in order to monitor both out- and in-diffusion processes. The furnace temperature changes slightly during the switching of ambient gases due to different heat capacity and flow rate from He. We note that excluding the initial curvature, the resistivity during He annealing is linear with time which in turn should be proportional to the oxygen loss. The precipitous drop of resistivity upon the introduction of air suggests that oxygen in diffusion is very fast in the oxide. The details of oxygen diffusion properties are discussed in a separate paper.<sup>11</sup>

In Fig. 3, the residual resistivity  $\rho_0$  extrapolated from the linear region at high temperature (from Fig. 1) is plotted as a function of oxygen deficiency  $\delta$ . Those data points with vertical error bars show the region of negative TCR at lower temperatures. In such samples, the extrapolation does not make much physical sense. However, the points are included to show the trend observed. Again, we note that  $\rho_0$  is linearly dependent on oxygen deficiency except for very small  $\delta$ .

Room-temperature powder x-ray diffraction measure-

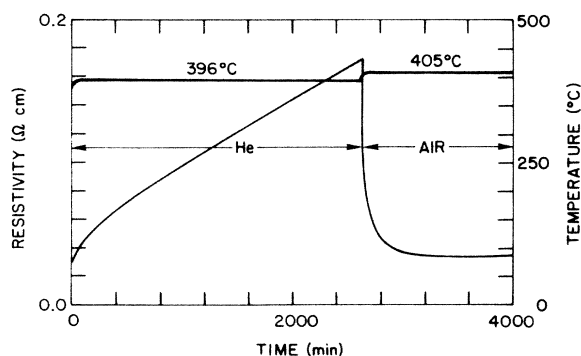


FIG. 2. The resistivity as a function of annealing time in different ambient environment. The annealing temperature is 396 °C.

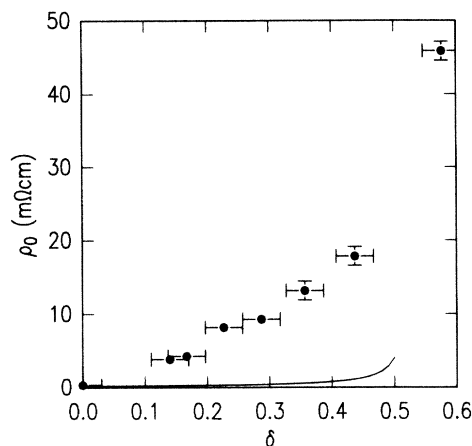


FIG. 3. The residual resistivity  $\rho_0$  as a function of oxygen deficiency  $\delta$ .  $\rho_0$  is obtained by extrapolating the linear portion of  $\rho$  vs  $T$  curve to zero temperature. The solid line is the contribution from the first term in Eq. (1).

ments were performed on the He-annealed samples, and the resulting lattice spacings are plotted as a function of  $T_c$  (defined at midpoint) in Fig. 4. The data points are generated by fitting at least nine high-angle diffraction peaks and by minimizing the  $\chi^2$ . In Fig. 4, the solid lines are drawn in to guide the eye. Note that  $a$  and  $b$  stay roughly constant as  $T_c$  decreases from 91 to 77 K and then vary smoothly with decreasing  $T_c$  while  $c$  increases in a nonmonotonic manner with decreasing  $T_c$ . We note that it is quite surprising to observe that the  $c$  axis expands upon losing oxygen from the  $a$ - $b$  plane.

We have also studied a few oxygen-deficient samples using low-temperature magnetic-susceptibility measurements. Briefly, we found that the  $T_c$ , as indicated by Meissner (or diamagnetic shielding) signals, decreases with He annealing, suggesting that the drop in  $T_c$  is a

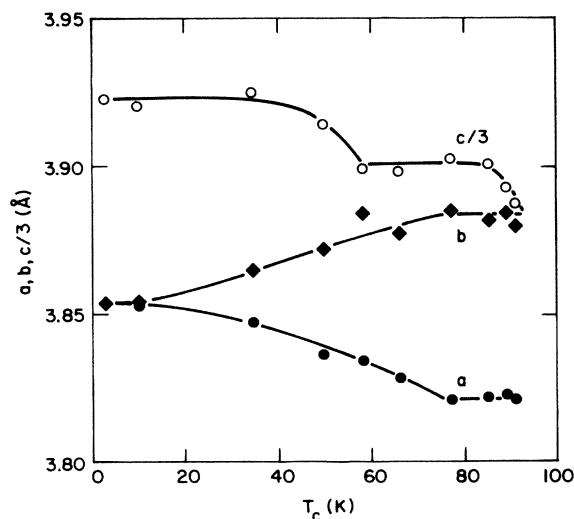


FIG. 4. The lattice spacings for  $a$ ,  $b$ , and  $c/3$  for samples with different  $T_c$ . The solid lines are provided to guide the eye.

bulk effect. In addition, the samples with  $[O] < 6.5$  which show a complete resistive superconducting transition exhibit a very small ( $< 5\%$  of the theoretical value) Meissner signal, indicative of its filamentary nature similar to the undoped  $\text{La}_2\text{CuO}_4$ .<sup>12</sup>

Regarding the behavior of the normal-state resistivity with oxygen loss, three features are noteworthy: first, the linear  $\rho$  vs  $T$  data (Fig. 1), second, the linear behavior of  $\rho$  with annealing time (Fig. 2) and with  $\delta$  (Fig. 3), and third, the appearance of negative TCR (Fig. 1). A model based on 1D conduction can explain all the above properties consistently. According to Bloch *et al.*,<sup>13</sup> the conduction in 1D conductors at high temperature ( $\sim 300$  K) is diffusive, with a conductivity determined by the Einstein equation,

$$\sigma = (Nne^2/kT)\langle\omega_0\rangle\langle(x_i - x_j)^2\rangle,$$

where  $N$ ,  $n$ , and  $x_i$  are the number of chains per unit cross-sectional area, the electron density on the chains, and the location of site  $i$ , respectively. If we assume that all the holes are located in the chain ( $Nn = 5.9 \times 10^{21}$  states/cm<sup>3</sup>), and  $\langle(x_i - x_j)^2\rangle$  is of order  $a^2$  while  $\omega_0$  is assumed to result from an Einstein mode at 20 mV,<sup>14</sup> the above equation yields  $d\rho/dT$  of  $2 \mu\Omega \text{ cm K}^{-1}$ , the value typically observed in polycrystalline  $\text{YBa}_2\text{Cu}_3\text{O}_7$ .<sup>15</sup> In order to compensate for the uncertainty in the resistivity owing to the inexact values of the geometrical factors and different sample processing, we compare the quantity  $\alpha = (1/\rho)(d\rho/dT)$  with the experimental data. The calculated value yields  $\alpha = 2.8 \times 10^{-3} \text{ K}^{-1}$  for  $\rho(T=0) = 100 \mu\Omega \text{ cm}$ . For various samples prepared by different groups including a single crystal<sup>9</sup> (measured for the  $a$ - $b$  plane),  $\alpha$  is in the range of  $2.5$ – $3 \times 10^{-3} \text{ K}^{-1}$ . We point out that the linear  $\rho$  vs  $T$  relation at high temperature can be generalized to systems other than 1D as long as the diffusive conduction between localized states is phonon assisted.

As the sample loses oxygen from the chain, the average length of unbroken CuO chains decreases. Since in 1D, any amount of disorder creates localized states, the wave functions will be localized to within each unbroken CuO chains. At high enough temperatures the thermal diffusion length  $l_t = (\hbar D/kT)^{1/2}$ , where  $D$  is the carrier diffusion constant, is smaller than the average chain length for  $\delta < \sim 0.3$ ,<sup>16</sup> and the conduction is metalliclike as described in the previous paragraph. As  $T$  is lowered,  $l_t$  gets larger than the average chain length, and the conduction has to occur through variable range hopping. Thus, the negative TCR in Fig. 1 can be explained. However, unlike the typical 1D conductors which preserve the anisotropic nature even in the presence of weak disorder, this system should assume an isotropic 3D variable range hopping once a large number of oxygen atoms is missing from the chain direction; the decay of wave function centered on a CuO chain of finite length should be more or less isotropic since the distance to the nearest Cu atoms is comparable in all three lattice directions. In such a case, the exponent of  $\frac{1}{4}$  should adequately describe the activated conduction<sup>17</sup> (inset of Fig. 1).

In order to understand the linear dependence of the resistivity on  $\delta$ , we consider the following equation to generally describe the total resistivity we measure at a given

temperature,

$$\rho_{\text{total}} = \frac{\rho_{7.0}}{n_{c0} + (1 - 2\delta)} + \rho_a. \quad (1)$$

The first term on the right-hand side represents the dependence of resistivity on the hole concentration and the second term the sum of additional sources of resistivity. The parameter  $n_{c0}$  denotes a small but finite carrier density which prevents a singular behavior at  $\delta = 0.5$ , and  $\rho_{7.0}$  is the resistivity for the  $[O] = 7.0$  sample. The use of  $n_{c0}$  is consistent with a two-band model.<sup>18</sup> If the role of the oxygen atoms in the CuO chains is to just regulate the number of holes, the first term should adequately describe the experimental result. In Fig. 4, the solid line is the contribution from the first term in Eq. (1) for  $\rho_{7.0} = 100 \mu\Omega \text{ cm}$  and  $n_{c0} = 0.05$ . The large difference between the solid line and the data shows that the reduction of holes is not the dominant effect. A possible source for the fast increase of  $\rho$  is the grain boundary phase<sup>19</sup> which becomes insulating and provides a large series resistivity. Another is the modification of band structure near the Fermi level. Yet, in both cases, it would be highly coincidental to obtain a linear relation between the total resistivity and  $\delta$ .<sup>20</sup> On the other hand, if we assume that the dominant conduction path is along the 1D CuO chains and there exists a large conductance anisotropy in all three directions, the carrier has to make a costly jump (in terms of resistivity since the jumps have to be along the direction of low conductivity) around every oxygen vacancy to either the neighboring chains or CuO planes. Since the resistivity is dominated by the least conductive paths and since the number of jumps should be proportional to the number of vacancy  $\delta$ , the resistivity should be proportional to  $\delta$  as observed. From Fig. 4 the slope  $d\rho_0/d\delta$  is  $\sim 40 \text{ m}\Omega \text{ cm/O}$  atom which means that if all the chains are removed, the sample will have a resistivity of about  $40 \text{ m}\Omega \text{ cm}$  (neglecting other effects such as band modifications). This resistivity is on the order of what Tozer *et al.*<sup>9</sup> measured for the resistivity ( $\sim 15 \text{ m}\Omega \text{ cm}$ ) in a single-crystal sample along the  $c$  direction. The measured resistivity could mean two things. First, it could mean that the in-plane resistivity becomes so large with oxygen vacancy that conduction occurs as a percolation process through the crystallites with  $c$  orientation. Or it means that the in-plane resistivity becomes comparable to that for  $c$  direction, and the conduction becomes isotropic. In view of the isotropic variable range hopping we observe (evidenced by the power of  $\frac{1}{4}$ ), we believe the latter is closer to reality. In both cases, it means that the conductivity associated with 2D CuO sheets is low, and that the in-plane conductivity should exhibit anisotropy of  $\sim 100$ . The lack of experimental observation of an anisotropy factor in  $a$ - $b$  plane can be attributed to the combined effects of twinning in the  $a$ - $b$  plane<sup>9</sup> and imperfect ordering of chains even in  $[O] = 7$  samples.<sup>4</sup>

Much work already exists on how  $T_c$  decreases rapidly with  $\delta$ . We now briefly comment on the superconducting properties. First, with the identification of the CuO chains as the dominant normal-state conduction channel in the previous paragraphs, we believe that the CuO chain is directly responsible for the superconductivity at 91 K.

Second, we note that the samples (numbered 5–7 in Fig. 1) become multiphase with He annealing. From the x-ray diffraction data, we do not observe any additional phases after He annealing. We do observe a gradual transition from orthorhombic to tetragonal structure (Fig. 4) as  $\delta$  changes from 0 to 0.7 in contrast to a sharp transition at  $\delta=0.5$  observed at higher temperatures. Therefore, we believe that the different phases correspond to regions of different crystal structure owing to the random distribution of O atoms and vacancies along the chain direction. By associating the well-defined resistivity drops at 45 and 77 K (Fig. 1) with superconductivity in these phases, we note that superconductivity depends strongly and exclusively on the local atomic configuration. We speculate that global superconductivity sets in when these independently superconducting substructures merge together physically or through electronic coupling. The monotonic increase of  $T_c$  with decreasing  $c$  lattice spacings for the  $T_c$  range of 77–91 K (Fig. 4) can be an indication of such a coupling process for 1D chains. Thus the oxygen atoms not only make up the linear chains but also provide couplings between different low-dimensional structural entities. This picture is consistent with the recent fluctuation results.<sup>21</sup> It is well known that true superconductivity cannot exist in strictly 1D system, and that only through interchain coupling is a 3D bulk superconductivity estab-

lished.<sup>22</sup> We also point out that this picture of superconducting substructures within an insulating matrix is a microscopic analog of granular systems consisting of superconducting grains imbedded in insulating matrix. In this regard we can explain the anomalous tunneling results<sup>23</sup> (superconducting grain sizes estimated from Gievers-Zeller tunneling formula were unrealistically smaller than the grain size) and the superconducting spin-glass-like behavior observed in magnetic-susceptibility measurements.<sup>24</sup>

In conclusion, a conduction in quasi-1D system can account for the behavior of the normal-state resistivity as a function of oxygen content. By associating the superconductivity with the dominant normal-state conduction channel, we conclude that superconductivity at 91 K is one-dimensional in nature associated with CuO chains. We speculate that bulk superconductivity in this material results as distinct, individually superconducting substructures couple together. The superconductivity in the substructures depends most crucially on the local atomic arrangements and has a well-defined  $T_c$  at 45 and 77 K.

The authors acknowledge useful discussions with C. C. Chi and R. Greene and thank J. Berosh for sample preparation.

<sup>1</sup>J. G. Bednorz and K. A. Muller, *Z. Phys. B* **64**, 189 (1986).

<sup>2</sup>See, for example, *Novel Superconductivity*, Proceedings of the Conference of Novel Mechanisms of Superconductivity, Berkeley, CA, 1987, edited by S. A. Wolf and V. Z. Kresin (Plenum, New York, 1987).

<sup>3</sup>J. D. Jorgensen, M. A. Beno, D. G. Hinks, L. Soderholm, K. J. Volin, R. L. Hitterman, J. D. Grace, I. K. Schuller, C. V. Segre, K. Zhang, and M. S. Kleefisch (unpublished).

<sup>4</sup>S. LaPlaca (private communication).

<sup>5</sup>J. van den Berg, C. J. van der Beek, P. H. Kes, G. J. Nienwenhuys, J. A. Mydosh, H. W. Zandbergen, F. P. F. van Berkel, R. Steens, and D. J. W. Ijdo (unpublished).

<sup>6</sup>N. P. Ong, Z. Z. Wang, J. Clayhold, J. M. Tarascon, L. H. Greene, and W. R. McKinnon (unpublished).

<sup>7</sup>P. Monod, M. Ribault, F. D'Yvoire, J. Jegoudez, G. Collin, and A. Revcolevschi *J. Phys. (Paris)* (to be published).

<sup>8</sup>R. J. Cava, B. Batlogg, C. H. Chen, E. A. Rietman, S. M. Zahurak, and D. Werder (unpublished).

<sup>9</sup>S. W. Tozer, A. W. Kleinsasser, T. Penney, D. Kaiser, and F. Holtzberg, *Phys. Rev. Lett.* **59**, 1768 (1987).

<sup>10</sup>P. K. Gallagher, H. M. O'Bryan, S. A. Sunshine, and D. W. Murphy, *Mater. Res. Bull.* **22**, 995 (1987).

<sup>11</sup>K. N. Tu, S. I. Park, and C. C. Tsuei, *Appl. Phys. Lett.* **51**, 2158 (1987).

<sup>12</sup>P. M. Grant, S. S. P. Parkin, R. L. Greene, V. Y. Lee, E. M. Engler, M. L. Ramirez, J. E. Vazquez, G. Lim, and R. D.

Jacowitz, *Phys. Rev. Lett.* **58**, 2482 (1987).

<sup>13</sup>A. N. Bloch, R. B. Weissman, and C. M. Varma, *Phys. Rev. Lett.* **28**, 753 (1972).

<sup>14</sup>R. T. Collins, Z. Schlesinger, R. H. Koch, R. B. Laibowitz, T. S. Plaskett, P. Freitas, W. J. Gallagher, R. L. Sandstrom, and T. R. Dinger, *Phys. Rev. Lett.* **59**, 704 (1987).

<sup>15</sup>R. J. Cava, B. Batlogg, R. B. van Dover, D. W. Murphy, S. Sunshine, T. Siegrist, J. P. Remeika, E. A. Reitman, S. Zahurak, and G. P. Espinosa, *Phys. Rev. Lett.* **58**, 1676 (1987).

<sup>16</sup>S. I. Park (unpublished).

<sup>17</sup>N. F. Mott, *Philos. Mag.* **19**, 835 (1969).

<sup>18</sup>J. Ihm and D. H. Lee, *Solid State Commun.* **62**, 811 (1987).

<sup>19</sup>R. A. Camps, J. E. Evetts, B. A. Glowacki, S. B. Newcomb, R. E. Somekh, and W. M. Stobbs (unpublished).

<sup>20</sup>Although granular tunneling may not explain the linear behavior, we believe it may be responsible for the initial curvature in  $\rho$  versus time plot in Fig. 3.

<sup>21</sup>P. P. Freitas, C. C. Tsuei, and T. S. Plaskett, *Phys. Rev. B* **36**, 833 (1987).

<sup>22</sup>L. P. Gorkov, *Prog. Low Temp. Phys.* **7B**, 517 (1978).

<sup>23</sup>J. R. Kirtley, W. J. Gallagher, Z. Schlesinger, R. L. Sandstrom, T. R. Dinger, and D. A. Chance, *Phys. Rev. B* **35**, 8846 (1987).

<sup>24</sup>Y. Yeshurun, I. Felner, and H. Sompolinsky (unpublished).